

Generation of Higher Frequency Components for Wind Gust by Fusion Analyses of WRF and LES –Cases of CBL, Tornado and Urban Canopy Flow

M. Kawaguchi¹, T. Tamura¹, T. Tao¹ and H. Kawai¹

¹Department of Architecture and Building Engineering
Tokyo Institute of Technology, Nagatsuta 4259, Yokohama, 225-0003, Japan

Abstract

Wind gust near the ground is turbulent flow and for the estimation of wind disaster risk, the peak velocity acting on buildings and structures has to be correctly predicted. In the case of meteorological model, the velocity fluctuations have a tendency of smoother variation without the high frequency component due to the filtering effects. In order to predict the peak velocity of wind gust with good accuracy, fully-developed turbulent flow is needed from the wind engineering point of view. In this paper, we propose a method for calculation of the higher frequency components of velocity and temperature fields of meteorological model using large eddy simulation (LES). The present method can regenerate broad-banded turbulent flows in wind gust and utilized for the fusion analysis of LES and meteorological model. We describe the result improvement of an actual extreme weather event of tornado by this fusion analysis. Also, we performed a simulation over urban area model using the flow detailed by the fusion analysis as inflow turbulence.

Introduction

Strong localized winds such as tornadoes and downbursts cause devastating disasters. They occur in almost all regions around the world and deprive human lives and cause severe damage on public and personal properties.

It is desired that numerical simulation provides meteorological knowledge of severe local storms. However, there are few successful simulation reports of tornado and other severe localized winds on actual weather condition by meteorological model. One of the reasons is inexistence of valid sub-grid scale turbulence scheme for numerical simulation in resolution between approximately 1 km and 100 m, known as “grey zone” of the atmospheric boundary layer [5], where both of three-dimensionality of turbulence and anisotropic property are significant. One potent strategy is to carrying out LES based on the flow and thermal field of meteorological data, because it is necessary in case of tornado and other localised strong wind events to carry out calculation of fine structure of flow field with high resolution grids and reliable numerical scheme including appropriate thermal effect consideration. Also, the detailed meteorological field with regenerated high frequency component is expected to useful to engineering application such as risk assessment and disaster mitigation in urban or residential areas.

In this paper, we propose a method for generating the higher frequency fluctuating component of flow and thermal field of meteorological model by LES and report the analysis of actual tornado process using the present method after validation in convective boundary layer. Also, we calculate flow field in urban area using flow field with reproduced high frequency component.

Calculation of Higher Frequency Fluctuating Component of Meteorological Model

We developed the calculation method by applying the formulation proposed by Nozawa and Tamura [3] for the equation of higher frequency fluctuating component of velocity field to thermal field so that atmospheric stability of actual weather has proper effect to the flow field.

Velocity Field

In one calculation domain where density deviation from static equilibrium is small, we can approximately describe velocity fields solved by coarser grids of meteorological model and finer grids of LES, \tilde{U}_i , \bar{U}_i respectively, by filtered Navier–Stokes equations.

$$\frac{\partial \tilde{U}_i}{\partial t} + \frac{\partial \tilde{U}_i \tilde{U}_j}{\partial x_j} = -\frac{\partial \tilde{P}}{\partial x_i} - \frac{\partial \tilde{\tau}_{ij}}{\partial x_j} + \beta(\tilde{\theta} - \theta_e)g\delta_{i3} \quad (1)$$

$$\frac{\partial \bar{U}_i}{\partial t} + \frac{\partial \bar{U}_i \bar{U}_j}{\partial x_j} = -\frac{\partial \bar{P}}{\partial x_i} - \frac{\partial \bar{\tau}_{ij}}{\partial x_j} + \beta(\bar{\theta} - \theta_e)g\delta_{i3} \quad (2)$$

where, $\tilde{\tau}_{ij} = \tilde{U}_i \tilde{U}_j - \tilde{U}_i \tilde{U}_j$, $\bar{\tau}_{ij} = \bar{U}_i \bar{U}_j - \bar{U}_i \bar{U}_j$: Reynolds stress terms. Other quantities with a tilde or an overbar are grid scale (GS) components filtered with respective grid systems. \tilde{P}, \bar{P} : GS pressure components, $\tilde{\theta}, \bar{\theta}$: GS potential temperature components. Thermal effect is introduced to the velocity field by Boussinesq approximation. θ_e : reference potential temperature, $\beta \cong 1/\theta_e$: coefficient of thermal expansion. Since the eddy diffusion is much larger than molecular diffusion, the molecular diffusion term is neglected in the formation.

Here, we define sub-grid scale (SGS) component of \tilde{U} as $u \equiv \tilde{U} - \bar{U}$. Then the partial component of u that is resolved by the finer grids corresponds to u filtered with the finer grid system and it can be denoted as \bar{u} . Relationship between the velocity components are shown in figure 1.

If the grid ratio of coarser grid size $\tilde{\Delta}$ to finer grid size $\bar{\Delta}$ is adequately large, the component \bar{u} satisfies the following expression.

$$\bar{u} = \overline{\tilde{U} - \bar{U}} = \bar{U} - \bar{\bar{U}} \cong \bar{U} - \bar{\tilde{U}} \quad (3)$$

Therefore, equation for the higher fluctuating component resolved by the finer grid \bar{u} is expressed as the difference of the two filtered Navier–Stokes equation of \bar{U} and $\bar{\tilde{U}}$.

$$\begin{aligned} \frac{\partial \bar{u}_i}{\partial t} + \frac{\partial}{\partial x_j} (\bar{U}_i \bar{U}_j - \bar{\tilde{U}}_i \bar{\tilde{U}}_j) = & -\frac{\partial}{\partial x_i} (\bar{P} - \bar{\tilde{P}}) \\ & - \frac{\partial}{\partial x_j} (\bar{\tau}_{ij} - \bar{\tilde{\tau}}_{ij}) + \beta(\bar{\theta} - \bar{\tilde{\theta}})g\delta_{i3} + f_i \end{aligned} \quad (4)$$

where, f_i is the feed-back forcing term based on method proposed by Goldstein et al. [2] so that the time average of \bar{u}_i is set to converge to 0. This term is expected to reduce the error arising from discrepancy of equation for the velocity component \tilde{U}_i in meteorological model and that is assumed in this method as equation (1). The above equation is solved for \bar{u} with \tilde{U} given by the meteorological model. Finally, we can acquire the detailed

flow field adding generated fluctuation to the original meteorological field.

For the Reynolds stress terms, τ_{ij} , which represents momentum influx from the meteorological field to the resolvable higher frequency component, is modeled by scale similarity model proposed by Bardina et al. [1] as $\tau_{ij} = \widetilde{U_i U_j} - \widetilde{U_i} \widetilde{U_j}$. On the other hand, $\bar{\tau}_{ij}$, which represents momentum efflux to even higher frequency component, is modeled by Smagorinsky model as $\bar{\tau}_{ij} = 2\nu_{SGS} \bar{D}_{ij}$. Scale similarity model has been proved to be good representation of SGS component by a priori tests, in spite of numerical instability. In this method, scale similarity model is utilized together with Smagorinsky model, which represents averaged energy dissipation well, and we overcome the drawback. Besides scale similarity model follows a natural assumption of energy continuity between GS and SGS component. It is expected to fit fairly even near the grey zone.

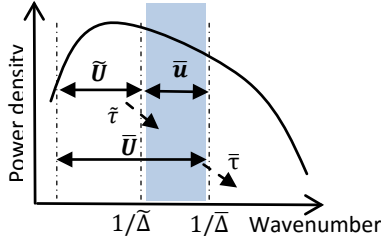


Figure 1 Energy spectrum of turbulence

Thermal Field

Similar to velocity field, we assume that potential temperature solved with meteorological model $\bar{\theta}$ and LES $\bar{\theta}$ satisfy transportation equations filtered with their grid systems.

$$\frac{\partial \bar{\theta}}{\partial t} + \frac{\partial \bar{\theta} \bar{U}_j}{\partial x_j} = -\frac{\partial \bar{h}_j}{\partial x_j} \quad (5)$$

$$\frac{\partial \bar{\theta}}{\partial t} + \frac{\partial \bar{\theta} \bar{U}_j}{\partial x_j} = -\frac{\partial \bar{h}_j}{\partial x_j} \quad (6)$$

where, $\bar{h}_j = \bar{\theta} \bar{U}_j - \bar{\theta} \bar{U}_j$ and $\bar{h}_j = \bar{\theta} \bar{U}_j - \bar{\theta} \bar{U}_j$; SGS heat fluxes

Given SGS component of the meteorological model potential temperature $\bar{\theta}$ is defined as $\bar{\theta} (\equiv \theta - \bar{\theta})$, we denote the partial component of θ that is resolved by the finer grids as $\bar{\theta}$, since this corresponds to θ filtered with the finer grids.

Since the component $\bar{\theta}$ satisfies the following relation

$$\bar{\theta} = \bar{\theta} - \bar{\theta} = \bar{\theta} - \bar{\theta} \cong \bar{\theta} - \bar{\theta} \quad (7)$$

Finally, we get

$$\frac{\partial \bar{\theta}}{\partial t} + \frac{\partial}{\partial x_j} (\bar{\theta} \bar{U}_j - \bar{\theta} \bar{U}_j) = -\frac{\partial}{\partial x_j} (\bar{h}_j - \bar{h}_j) \quad (8)$$

For SGS heat fluxes, \bar{h}_j is modeled by scale similarity model ($\bar{h}_j = \bar{\theta} \bar{U}_j - \bar{\theta} \bar{U}_j$) and \bar{h}_j by Smagorinsky model ($\bar{h}_j = \nu_{SGS} / k_{SGS} \partial \bar{\theta} / \partial x_j$), where k_{SGS} is turbulent Prandtl number.

Numerical Schemes and Conditions

Table 1 shows numerical schemes for the domain of the couple analysis. As for boundary condition, either the fluctuating component or its gradient is set to be 0.

Spatial discretisation	Velocity: 4 th order central difference Heat: 2 nd order central difference
Time marching	2 nd order Adams–Bashforth method
Pressure solver	SOR method
Grid ratio $\bar{\Delta}/\bar{\Delta}$	2.0

Table 1. Numerical schemes and conditions for coupled analysis

Numerical Validation in Convective Boundary Layer

An ideal convective boundary layer (CBL) was simulated in 25m resolution and filtered into 50m resolution. Then we carried out regeneration of higher frequency component in 25m resolution again by the method proposed in the previous section. CBL was calculated by WRFLES in the domain under periodic boundary condition with 10m initial wind set across the domain. Other domain settings are shown in figure 2.

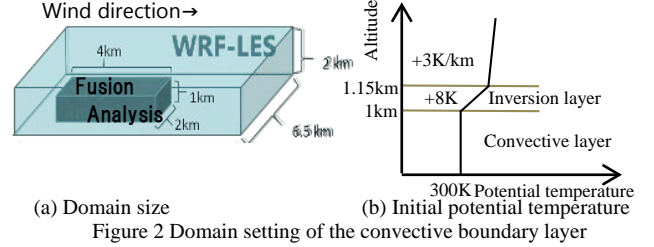


Figure 3 shows instantaneous velocity and potential temperature fields in horizontal cross-sections at an altitude of 500m. Both higher frequency components of velocity and heat was generated. Comparison of the original CBL by WRFLES and regenerated CBL reveals that regenerated components does not much completely to the original in this case. However, for flow field, turbulent structure converged and finer structure regenerated across the domain. For thermal field, although absolute value of the generated fluctuation of temperature was very small, structure in thermal field slightly converged and became clearer. Discrepancy of the reproduced and original CBL may be attributed to the difference in formulation of the component $\bar{\theta}$ and $\bar{\theta}$ in meteorological model and proposed method. The result could be improved if better regeneration of fluctuating temperature is realized optimising arbitral parameters in the model. A priori test based on LES will also be conducted for next validation step.

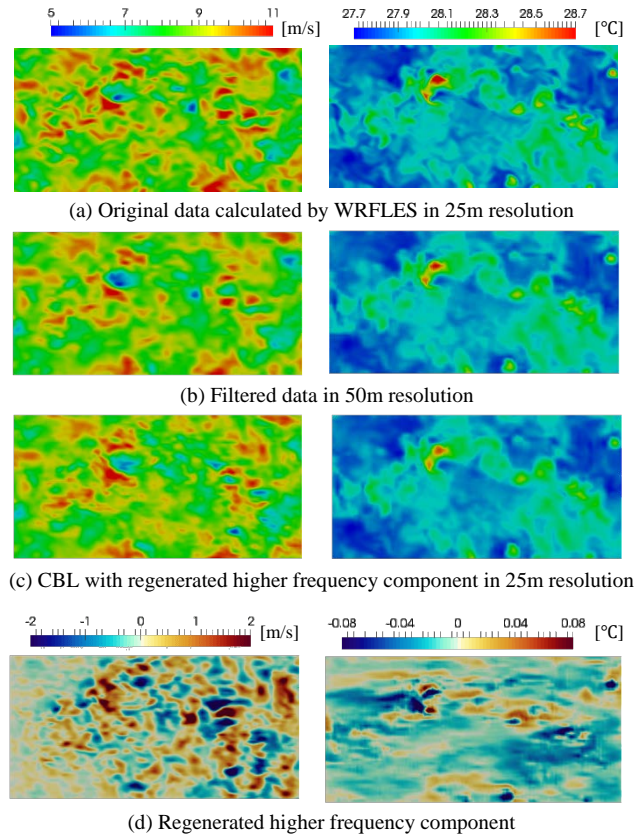


Figure 3. Instantaneous velocity (left) and potential temperature (right) fields of CBL in horizontal cross-sections at an altitude of 500m

Coupled Simulation of Tornado Under Actual Meteorological Conditions

Prediction of maximum velocity occurring at tornado is very important for safety to disaster due to extreme wind gust. However, the data about maximum velocity have not been obtained since the wind velocity measurement is very difficult at tornado. This study tried to carry out the simulation of the actual tornado which occurred at Tsukuba in Japan at May 2012. The fusion method proposed in the previous chapter was applied to the extreme event by the actual Tsukuba tornado. First the WRF simulation was performed using the horizontal mesh with 250m and produced the basic data for the fusion analysis. Next, the fusion simulation is carried out by solving the equation of higher frequency components of velocity and potential temperature. The fusion simulation employed the computational domain of 20km square with the 125m mesh resolution. In the vertical direction, the range with 200m altitude to 1800m altitude is analyzed with twice finer mesh resolution of original mesh on WRF. WRF simulation conducted by Tao et al. [4] already have succeeded in the reproduction of various meteorological events. The strong supercell could be reproduced in unstable atmospheric condition and includes the mesocyclone generated inside. Mesocyclone extended straight to the ground and formed the tube structures of vertical vortex rotation. But this tube is simple and has no high frequency components.

Figure 4 shows the time series of the horizontal and the vertical velocities at 945 m height and the horizontally central point of the computational domain. In comparison between the results obtained by WRF and the fusion analysis, the large-scaled time variations of both the velocities fluctuates with the almost same phase pattern. But the fusion analysis shows the very sharp end around the peak indicated at the nearest tornado. The high frequency and the high wavenumber fluctuation are superimposed and recognized in the time series of velocities.

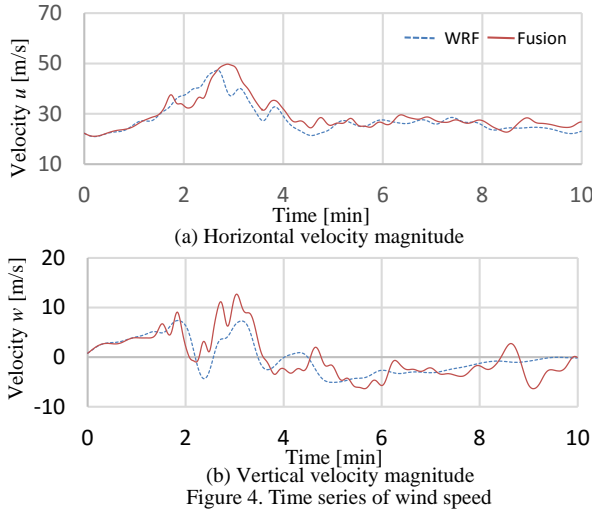


Figure 5 illustrates the instantaneous velocity contours on the horizontal section at 1km altitude obtained by WRF and the coupling analysis. The data-taken time is 5 minutes past after the start of simulation. The enlarged figures are included at upper right of each figure. The velocity components consist of west-to-east, vertical and north-to-south directions. Near the vortex center which can be determined by the horizontal velocity contours, the fusion analysis clearly elucidates the details of fine structures of the RFD as well as the up and down drafts. The intensification of the peak velocity of the up- and downdraft can be recognized more obviously. Also, it can be observed that the turbulence fine structures are

formed in the low velocity zone such as the streak structures on the vertical velocity component along or near the frontal line (equivalent to the boundary of positive and negative values of the vertical velocity).

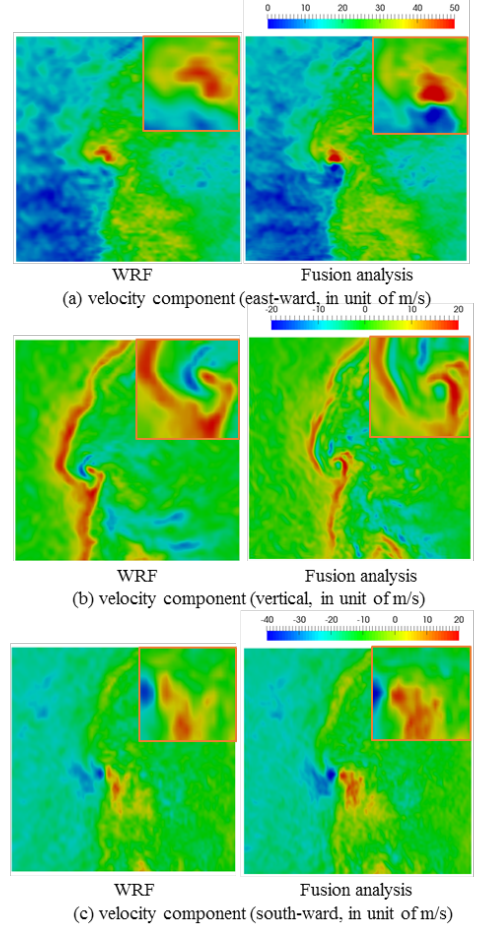


Figure 5. Comparison of instantaneous velocity components

Figure 6 depicts the flow visualization of tornado-like vortex and its surroundings. The direction of the moving of the vertical vortex is shown by the arrow. The contouring surfaces are shown by the Q values equivalent to the intensity of rotation of the vortex and colored by vertical component of the vorticity. At the same time the instantaneous vertical velocities at 224 m height are illustrated. In the case of the WRF, the vertical vorticity of the vortex becomes maximum value of 0.25 s^{-1} but the fusion analysis indicates the 0.5 s^{-1} as maximum vorticity with increasing the fluctuations. Also, the fusion analysis obviously clarify the structures of horizontal vortex occurring close to the frontal lines.

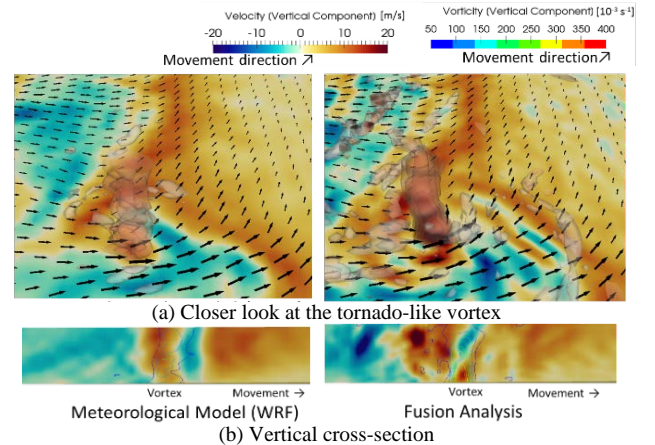


Figure 6. Tornado-like vortex and its surroundings

Figure 7 depicts the distributions of maximum vertical vorticity and contours of maximum horizontal velocity. The maximum values are obtained during all computational time of 10 minutes. In order to estimate the occurring risk of disaster by the extreme wind gust like a tornado, these data is used. By the maximum vorticity the tornado trace can be determined. The maximum horizontal velocity is definitely indicated on the right hand side of the tornado-moving direction. Investigating the disaster data for the houses attached by the actual Tsukuba tornado, the predictive level of the maximum velocity can be validated.

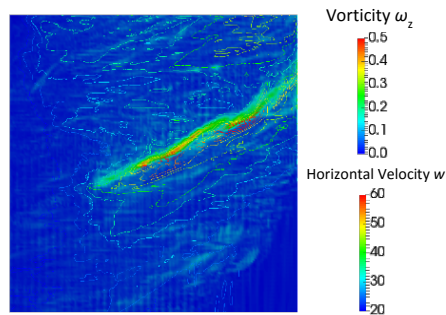


Figure 7. Distribution of maximum vertical vorticity
Iso-line shows maximum horizontal velocity.

Introduction of Fusion Analysis Results to an Urban Area Simulation

This study introduces the results of convective boundary layer which is obtained by the presented fusion analysis to an urban area computation. In the urban area computation, the geometry of 4×4 cube blocks assuming urban geometry is reproduced. The length of cube and its interval is 0.18 (approximately 65m). Detailed calculation conditions are shown in Table 2. In this computation, inflow turbulence is imposed on the region at the height of 246-675m in inlet surface because the fusion analysis is carried out in the region above the ground. The inflow turbulence has fine turbulent structures and fluctuation of velocity and temperature by the presented fusion analysis (figure 8). On the other hand, for the region at the height of less than 246m, the velocity and temperature is extrapolated from fusion analysis results in upper side (figure 9). This extrapolation is carried out with assuming the logarithmic law.

Figure 10 shows the velocity and temperature field at the time when 8 minutes passed. The introduced inflow structure flows to the area above urban blocks, and the turbulence is mixed with the structure generated from urban structures. Then, it is shown that convection vortex which is generated from heated surface of urban blocks and ground transports to upper side.

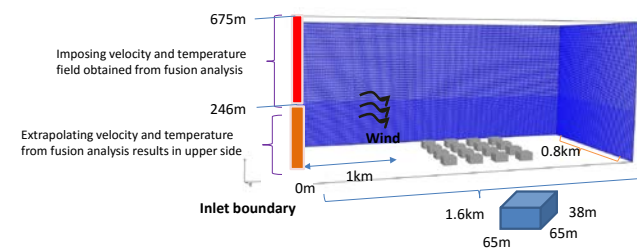


Figure8. Illustration of the calculation domain of urban model area

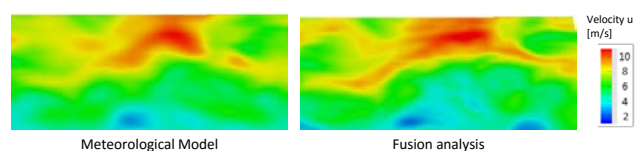


Figure 9. Fusion analysis of CBL

Domain	Streamwise: 2.48 (1560 m) Spanwise: 1.28 (780 m) Vertical: 1.038 (675 m)
Grid resolution	Horizontal: $\delta/100$ (6.5m)
Time increment	0.025s
Spatial discretisation	Velocity: 4 th order central difference Temperature: 2 nd order central difference
Time integration	2 nd order Adams–Bashforth
SGS model	Smagorinsky (Cs=0.20)

Table 2 Numerical schemes and calculation conditions

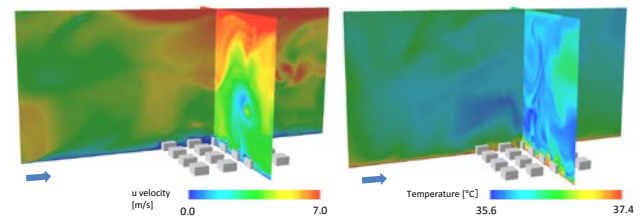


Figure 10. Velocity and temperature field in the urban area computation

Conclusions

We proposed a calculation method for generating higher frequency fluctuation component of meteorological models including thermal effect. Fluctuation was generated for both of velocity and potential temperature field.

As an analysis of an actual extreme weather condition, fusion analysis was applied to a case of tornado-like strong vortex. A variety of flow structure of vortex core and its surroundings was refined throughout the domain.

We also carried out analysis in LES with a simple urban area model introducing CBL inflow generated by fusion analysis. Flow field around buildings was solved under meteorological model simulation result.

References

- [1] Bardina, J., Ferziger, J.H. and Reynolds, W. C.: Improved subgrid scale models for large eddy simulation, *AIAA* , 80, 1357, 1980
- [2] Goldstein, D., Handler, R. and Sirovich, L., Modeling a no-slip flow boundary with an external force field, *J. of Comp. Phys.*, 105 , 354-366, 1993.
- [3] Nozawa, K., Tamura, T., LES one-way coupling of nested grids using scale similarity model, in the *Seventh International Symposium on Turbulence and Shear Flow Phenomena*, 2011
- [4] Tao T., Kawai H., Kawaguchi M., and TamuraT.: WRF Simulation of Severe Storm Process Focusing on the Characteristics of Extreme Local Gust near Ground, in *28th Conference on Severe Local Storms*, 2016
- [5] Wyngaard, J. C., Toward numerical modeling in the “Terra Incognita”, *Journal of the atmospheric sciences*, 61(14) 1816-1826, 2004